

Effect of Solvents on Interactions between Hydrophobic Self-Assembled Monolayers

Efrosini Kokkoli and Charles F. Zukoski¹

Department of Chemical Engineering, Beckman Institute for Advanced Science and Technology, University of Illinois at Urbana-Champaign, Urbana, Illinois 61801

Received March 31, 1998; accepted September 10, 1998

An atomic force microscope was used to measure forces between self-assembled monolayers (SAMs) of hexadecanethiol as a function of solvent type. Solvents alter interactions between surfaces by changing the wetting properties of the surface. Adhesive forces decrease with solvent dielectric constant and vary monotonically for mixtures of water and ethanol, ethanol and methanol, and water and ethylene glycol. This study demonstrates that interactions and adhesion between hydrophobic SAMs can be manipulated through changes in the contact angle of the surface. © 1999

Academic Press

Key Words: solvents; adhesion; self-assembled monolayers; wetting properties; atomic force microscope.

INTRODUCTION

Hydrophobic interactions have been invoked in the biochemical literature to explain the driving forces that govern a variety of molecular processes, including conformational changes of biopolymers, the binding of substrates to enzymes, and the association of subunits to form a multisubunit enzyme (1). Indeed a major driving force for the evolution of the whole field of study of hydrophobic interactions is the need to explain such processes in biological systems that cannot be explained by the conventional interactions between molecules or between groups within a molecule. Hydrophobic interactions are also important in many technological and industrially significant processes including wetting (2), froth flotation (3), deinking technology (4), and adhesion (5). Understanding these interactions remains limited and progress requires more experimental studies showing how forces depend on external parameters and surface properties.

Rabinovich and Yoon (6) and Yoon *et al.* (7) suggest that the hydrophobic force is uniquely determined by contact angles. Their results demonstrate that for different surfaces, interacting across an aqueous electrolyte, that exhibit different contact angles jump-in distances (a measure of the extent of attraction)

¹ To whom correspondence should be addressed at Department of Chemical Engineering, University of Illinois at Urbana-Champaign, 114 Roger Adams Laboratory, Box C-3, 600 South Mathews Avenue, Urbana, IL 61801.

and adhesion forces grow with increasing contact angle. Here we demonstrate that for the same set of hydrophobic surfaces, attractive interactions can be altered by changing the solvent across which the surfaces interact. As the solvent contact angle decreases, the adhesive force decreases. This behavior is distinct from that observed between the same surfaces interacting across electrolytes that do not alter the surface wetting properties (8).

Model hydrophobic surfaces should satisfy the double criteria of electroneutrality and stability, so that the resulting interactions can be easily interpreted. In this study we have chosen to work with self-assembled monolayers (SAMs) of hexadecanethiol, which satisfy both criteria. SAMs are robust, well-characterized, and easily prepared (9–16). SAMs represent an excellent model system as far as modifying surface characteristics in a molecularly rationalized way and have successfully been used in atomic force microscopy (AFM) measurements of adhesion forces and friction (17–19).

The focus of this paper is to characterize the interaction between hydrophobic surfaces by using an AFM and study how the magnitude of the adhesive force can be modified through changes in the surface wettability.

METHODS AND MATERIALS

Surface force measurements were performed using a commercial AFM, a Topometrix TMX 2010 (Topometrix, Santa Clara, CA). All experiments were carried out at room temperature. The data were converted to a force–distance curve using the method developed by Ducker *et al.* (20, 21).

Standard 100- μm V-shaped silicon nitride AFM cantilevers with pyramidal tips (Topometrix, Santa Clara, CA) were used for the force measurements. The colloid probe tips were prepared as follows. A glass sphere (SPI Supplies, West Chester, PA) of radius approximately 10 μm (the radius was measured by optical microscopy) was attached to the cantilever with an epoxy resin, Epon Resin 1004F (Shell Chemical, Houston, TX). A heated thin copper wire ($\sim 30 \mu\text{m}$ in diameter) attached to a three-axis translation stage was used to position a small portion of the glue near the apex of the cantilever. Another

clean wire was used to put a glass sphere onto the tip. The cantilever was heated just enough to melt the Epon and secure the particles in place.

Substrates of the desired size were cut from Si (100) wafers (WaferNet, San Jose, CA; test grade). These substrates and colloid probe tips were coated by thermal evaporation with 250–500 Å gold (99.999%; Alfa, Ward Hill, MA). Care was taken to avoid overheating the colloid probe tips or evaporating too much gold on them since in both cases the cantilevers bend. The spring constant of the gold-coated colloid probe tips was determined using the resonant frequency method (22). The spring constant was measured for 15 cantilevers and the average value was used (1.65 N/m).

Hydrophobic surfaces were prepared by forming SAMs of hexadecanethiol (Aldrich, Milwaukee, WI) on the gold-coated surfaces (10, 11, 16).

RESULTS AND DISCUSSION

The SAM surfaces were first characterized by using the colloid probe tip to image the substrate surface. For all systems, the substrate was smooth, showing large regions (70 by 70 μm) where the root-mean-square roughness was less than a nanometer. However, the glass spheres were relatively rough (8). On occasions and due to the presence of a sharp asperity on the colloidal probe, atomic resolution images were produced, permitting individual terminal methyl groups to be visualized. Care was taken to apply forces well below the reported load for monolayer damage (23). Figure 1A shows an AFM image of the thiol in 0.5 mol fraction ethylene glycol in water. This image was acquired with a 10- μm -radius probe that had been functionalized with the hexadecanethiol as well. Individual methyl groups of the hydrocarbon chain can be identified. The thiol forms a hexagonal lattice with a lattice constant of 5 Å, as shown in the cross-sectional profile (Fig. 1B) along the line drawn in the image, and is in agreement with the value reported in the literature (13–15, 23).

The interactions between SAM surfaces in solvents are purely attractive, with a jump into contact as the force gradient exceeds the spring constant. Due to the sharpness of the force/distance curves near contact, this distance is weakly sensitive to the spring constant used. The extent of the attraction must be measured relative to some force scale (i.e., the separation where the attractive force goes to zero). In our case, the force changes dramatically over a small change in separation. Under these circumstances the jump-in distance provides a qualitative measure of the extent of attraction. In the remainder of this paper we use the jump-in distance to characterize the extent of the attractive interactions. Note however that order of magnitude decreases in spring constant will greatly increase this characteristic length. Thus this method provides a relative rather than an absolute method of probing the extent of attractive forces. Representative force curves are shown in Fig. 2 for the ethanol–water system. In water, the thiol surfaces are

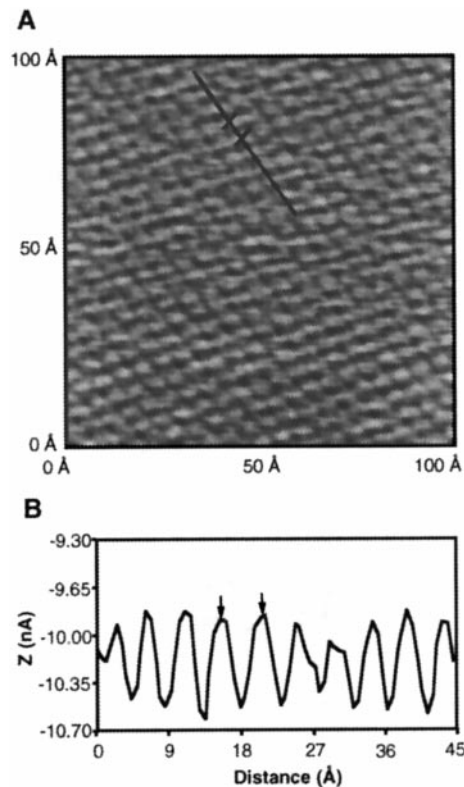


FIG. 1. (A) An AFM (lateral force mode) image of a hexadecanethiol SAM on gold in 0.5 mol fraction ethylene glycol in water. This image was acquired with a 10- μm -radius probe that had been functionalized with hydrophobic molecules (SAM of hexadecanethiol). Individual methyl groups of the hydrocarbon chains can be identified. A low pass filter was applied. (B) Cross-sectional profile along the line drawn in the image (the Z scale is in arbitrary units, cantilever deflection, nA). The two terminal groups associated with the hexadecanethiol molecule (as indicated by arrows) are separated by 5 Å.

pulled into an adhesive contact from a distance of 7.2 nm, and upon addition of 0.5 mol fraction ethanol, the jump to contact occurs at a surface separation of 3 nm. Figure 2 contains theoretical van der Waals curves for the case of water and ethanol. The nonretarded van der Waals force between two identical surfaces, 1, with adsorbed layers, 2, and across medium, 3, is given by the approximate expression (24)

$$\frac{F}{R} = \frac{-1}{6} \left[\frac{A_{232}}{D^2} - \frac{2\sqrt{A_{121}A_{232}}}{(D+T)^2} + \frac{A_{121}}{(D+2T)^2} \right], \quad [1]$$

where F is the van der Waals force, R is the radius of the sphere, D is the distance between the sphere and the flat surface, T is the thickness of the monolayer (2.2 nm), and A is the unretarded Hamaker constant. The index 1 corresponds to the gold surface, 2 to the hexadecanethiol SAM, and 3 to the medium. The Hamaker constants were calculated on the basis of the Lifshitz theory (24), and the following values were used

$A_{232} = 4.97 \times 10^{-21}$ J ($\beta = \text{water}$), $A_{232} = 3.28 \times 10^{-21}$ J ($\beta = \text{ethanol}$), and $A_{121} = 2.15 \times 10^{-19}$ J.

In Fig. 3, jump-in distances are given as a function of the ethanol mole fraction in water (x_{EtOH}). Each data point is the average of 10–15 force measurements and the error bars correspond to the standard deviations. As more ethanol is added to the solution, the interaction becomes of shorter range. The experimental jump-in distances are compared to those predicted by the classical van der Waals theory for two gold surfaces with hexadecanethiol SAMs interacting across water and ethanol. The theoretical van der Waals jump-in distance in ethanol is 2.05 nm and in water is 2.11 nm. Our data indicate that jump-in distances in water and small concentrations of ethanol are considerably larger than those predicted for our gold–SAM surfaces interacting across water or ethanol, indicating that the forces do not arise from van der Waals interactions. However, as the ethanol concentration is increased further (75% mole fraction), the jump-in distance becomes comparable to what is predicted by van der Waals attractions. In Fig. 3 the effect of hydrophobic forces is not observed in ethanol–water mixtures for $x_{\text{EtOH}} > 0.75$, where the interactions approach the van der Waals limit. This trend suggests that the solvophobic forces can be altered as the solvent is changed.

Shown in Fig. 4 are scaled pull-off forces as a function of ethanol mole fraction in water. The pull-off force or adhesion force is defined as the minimum force that must be applied to separate the two surfaces. The rate (0.5–2 Hz) at which the surfaces were separated or the time that the opposed surfaces rested in contact (50 μs –0.5 s) before the pull-off forces were applied did not have an effect on the magnitude of the adhesive forces. Here we present forces scaled by the radius of the sphere, R , in order to relate the force between a curved and a flat surface to the interaction free energy, E , between plane parallel plates of unit area by $F/R = 2\pi E$ (25).

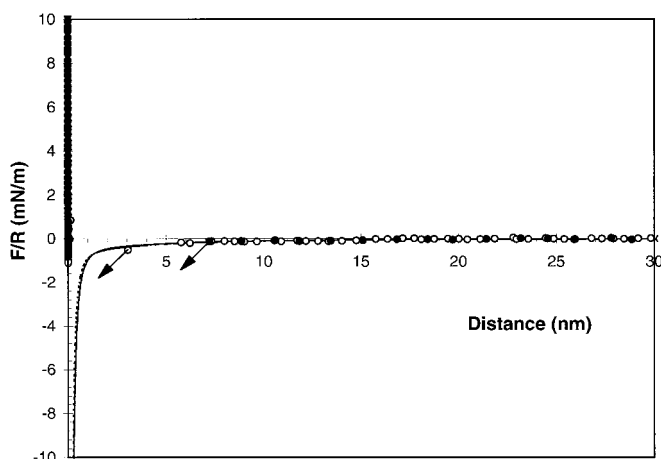


FIG. 2. Normalized forces recorded between SAMs of hexadecanethiol in water (●) and in 0.5 mol fraction ethanol in water (○). The arrows show the jump distances (7.2 nm in water and 3.0 nm in 0.5 mol fraction ethanol in water). The solid and dashed lines indicate fits to van der Waals theory, using Eq. [1], in water and ethanol, respectively.

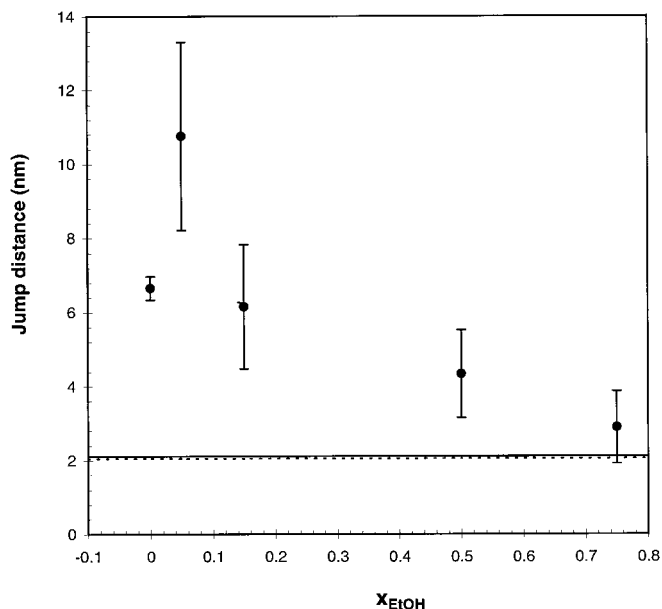


FIG. 3. Jump-in distances versus the mole fraction of ethanol in water for hexadecanethiol SAMs. The error bars correspond to the standard deviations that resulted from 10 to 15 force measurements all over the surface. The dashed and solid lines correspond to the van der Waals jump distances for gold–SAM surfaces in ethanol (2.05 nm) and gold–SAM surfaces in water (2.11 nm), respectively. Measurements were done with the same tip and surface as in Fig. 2.

Addition of ethanol to water results in a decrease in the strength of attraction and adhesion. In the case of the ethanol–water mixture, the surface tensions of pure water and pure ethanol differ appreciably ($\gamma_{\text{H}_2\text{O}} = 72.94$ mN/m and $\gamma_{\text{EtOH}} = 22.39$ mN/m at 20°C) (2). As a result, the addition of small amounts of ethanol results in a marked decrease in surface tension from that of the water. This effect may be accounted for in terms of a selective adsorption of the alcohol at the liquid–vapor interface.² The liquid–vapor surface tension of the ethanol–water solution decreases with increasing concentration of ethanol in a logarithmic fashion (2). The decrease in surface tension and therefore in the contact angle suggests that the surfaces become less solvophobic with increasing ethanol concentration. To confirm this, advancing contact angles of pure water and pure ethanol were measured on our surfaces. For water $\theta = 109^\circ \pm 1^\circ$ and for ethanol $\theta = 19^\circ \pm 2^\circ$. The contact angle measurements correlate well with the changes in adhesive forces as x_{EtOH} is altered, indicating that for these systems the interaction forces track the surface wetting properties. After forces were measured in 0.75 mol fraction ethanol, forces were again measured in pure water. Both the jump-in distance and the adhesive force were the same as those measured in water at the beginning of the experiment. Thus

² If the surface tension of a liquid is lowered by the addition of a solute, then, by the Gibbs equation, the solute must be adsorbed at the liquid interface. For a more extended discussion see Ref. (2).

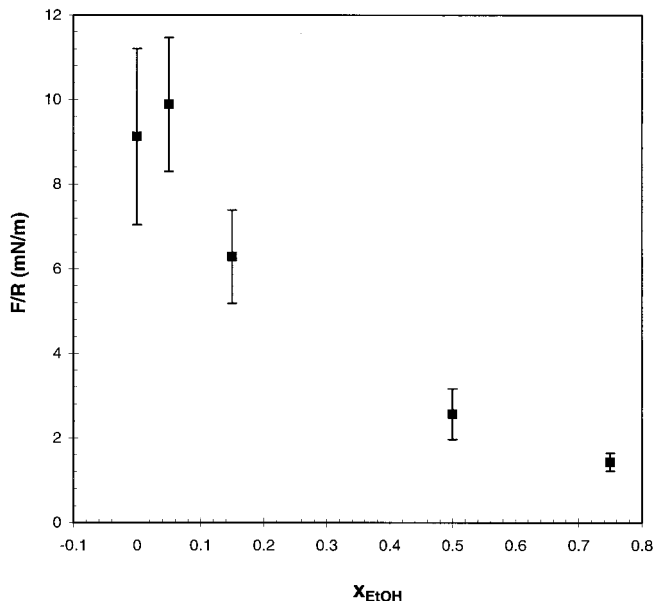


FIG. 4. Pull-off force/radius of sphere versus the mole fraction of ethanol in water for hexadecanethiol SAMs. The error bars correspond to the standard deviations that resulted from 10 to 20 force measurements all over the surface. Measurements were done with the same tip and surface as in Figs. 2 and 3.

changes in wetting properties and the resulting surface forces are reversible.

Figures 3 and 4 both exhibit a small maximum at a mole fraction of 0.05. Yaacobi and Ben-Naim (26) have measured the effect of ethanol on the work associated with the dimerization of methane molecules in an ethanol–water solvent. Their findings show that the addition of small quantities of ethanol up to about $x_{\text{EtOH}} \approx 0.2$ increases the strength of the hydrophobic interaction between small hydrocarbon molecules; larger ethanol mole fractions cause a weakening of the hydrophobic interaction. Our data show a maximum for mole fractions around 0.05: the addition of small quantities of ethanol ($x_{\text{EtOH}} \leq 0.05$) induces a small strengthening of the extent of attraction and adhesion that the two hydrophobic surfaces feel, whereas at higher concentrations of alcohol ($x_{\text{EtOH}} > 0.05$) there is a pronounced decrease.

If the JKR theory is used to calculate the surface energy corresponding to the adhesion force that we measure in water, it is only a few milliNewtons per meter, whereas the value that we calculate from Young's equation and the contact angle that we measure in water is approximately 40 mN/m.³ A serious though practical limitation of the JKR theory is that it assumes perfectly smooth surfaces, and although our sample surfaces are smooth, our spheres are not. The roughness of the sphere plays a significant role in the forces measured. For example, if

³ From Young's equation: $\gamma_{\text{SV}} - \gamma_{\text{SL}} = \gamma_{\text{LV}} \cos \theta$, where $\gamma_{\text{SV}} = 18$ mN/m (M. K. Chaudhury and G. M. Whitesides, *Langmuir* 7, 1013 (1991)), $\gamma_{\text{LV}} = 72.13$ mN/m (for water at 25°C (2)), and $\theta = 109^\circ$. From this, $\gamma_{\text{SL}} = 41.48$ mN/m.

we use the JKR theory and an asperity radius of $R = 0.45 \mu\text{m}$ (8), the surface energy is in the order of 36–40 mN/m. Asperities of this size are not uncommon on the glass sphere surfaces (8). This result clearly shows the sensitivity of adhesion to surface roughness and difficulties in comparing theoretical predictions with measurements.

Because the sphere surface is not smooth, comparisons of interaction forces in different solutions can be done only with the same tip and surface. For a given set of mixtures, the same tip and surface were used. However, different colloid probes and surfaces were used for the three different solvent mixtures investigated here. Therefore quantitative comparisons are difficult.

Our results for ethanol–water mixtures are in qualitative agreement with measurements of interaction of fluorocarbon surfaces (27, 28). Parker and co-workers showed that in water these surfaces are strongly hydrophobic with corresponding advancing and receding water contact angles of 108° and 90° , respectively. The addition of 0.23 mol fraction ethanol in water decreased the liquid–vapor surface tension, giving a contact angle of 63° , and decreased the strength of the long-range attraction and adhesion (from 240 mN/m in water to 56–63 mN/m at $x_{\text{EtOH}} = 0.23$).

In addition to ethanol–water mixtures, we have also measured the effect of addition of ethylene glycol and surface interactions across methanol–ethanol mixtures. Figure 5 shows the pull-off force scaled by the radius of the sphere for different mole fractions of ethylene glycol in water (x_{EG}). Behavior similar to that seen in the ethanol–water system is observed. The advancing contact angle changes from $\theta = 109^\circ \pm 1^\circ$ in pure water to $\theta = 83^\circ \pm 1^\circ$ in pure ethylene glycol and the

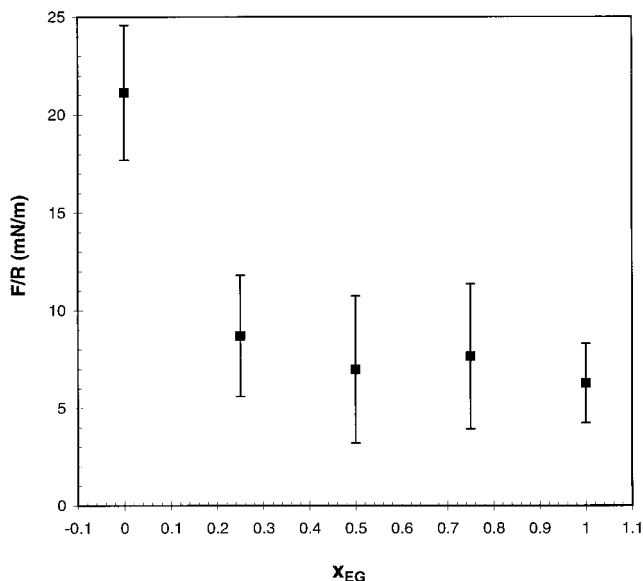


FIG. 5. Pull-off force/radius of sphere versus the mole fraction of ethylene glycol in water for hexadecanethiol SAMs. The error bars correspond to the standard deviations that resulted from 10 to 20 force measurements all over the surface.

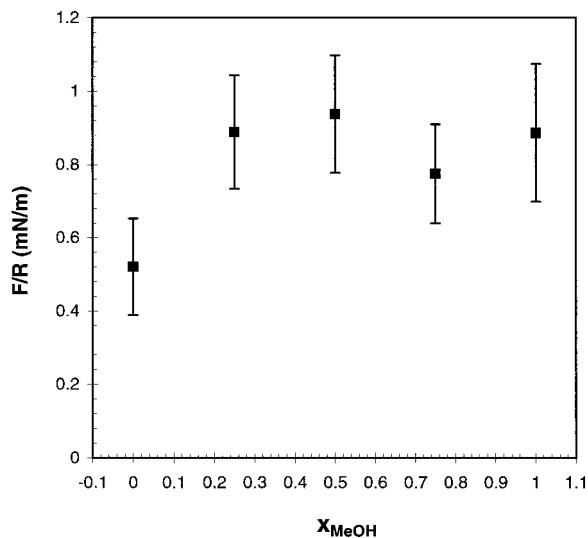


FIG. 6. Pull-off force/radius of sphere versus the mole fraction of methanol in an ethanol–methanol mixture for hexadecanethiol SAMs. The error bars correspond to the standard deviations that resulted from 10 to 20 force measurements all over the surface.

receding contact angle changes from $\theta = 96^\circ \pm 2^\circ$ to $\theta = 67^\circ \pm 2^\circ$. These results demonstrate that in ethylene glycol, SAM surfaces are less solvophobic than water. Adhesive forces decrease with increasing ethylene glycol mole fraction up to a value of 0.5. For $x_{\text{EG}} > 0.5$, the adhesion remains constant at one-third of the value in pure water. In addition as x_{EG} grows, jump-in distances decrease. In pure ethylene glycol the surfaces jump into an adhesive contact at a distance that is two-thirds of the value in pure water. However, these interactions remain larger and have a greater extent than can be predicted by van der Waals interactions alone. As a consequence, we conclude that solvophobic interactions exist in a nonaqueous solvent like ethylene glycol. This observation is similar to that reported by Tsao *et al.* (29) for interactions between double-chained cationic surfactants on mica interacting across ethylene glycol. Parker and Claesson (30) showed that interactions between two fluorocarbon surfactant monolayers measured against 51% ethylene glycol in water are almost identical to those observed between hydrophobic surfaces in water. Upon further increase of ethylene glycol content decreases in the range and strength of the attractive force are observed and forces between two fluorocarbon surfaces are comparable to those expected for van der Waals interactions in pure ethylene glycol.

Figure 6 shows the pull-off force scaled by the radius of the sphere for different mole fractions of methanol in a methanol–ethanol system showing a monotonic increase in the strength of adhesion between thiol surfaces as the methanol mole fraction is increased. This result can again be understood in terms of a reduction in contact angle. The contact angle of the solvent on the SAM is increased going from ethanol to methanol (for ethanol $\theta = 19^\circ \pm 2^\circ$ and for methanol $\theta = 22^\circ$ (12)). The thiol

surfaces are quite solvophilic in the presence of both ethanol and methanol. The adhesion measured between thiol SAMs in these solvents is small, which was expected for a set of surfaces that exhibit a higher affinity for the solvent than for each other. The jump-in distances are also small and, within the instrument sensitivity, there appears to be no obvious relationship between jump-in distances and the methanol mole fraction in ethanol with values that vary between 2 and 3 nm. The van der Waal theory predicts that two gold–SAM surfaces will jump into contact at a separation of 2.05 nm in ethanol and 2.10 nm in methanol, using Eq. [1] and an unretarded Hamaker constant of $A_{232} = 4.79 \times 10^{-21}$ J ($3 = \text{methanol}$), $A_{232} = 3.28 \times 10^{-21}$ J ($3 = \text{ethanol}$). Thus we can conclude that interactions between thiol SAMs in ethanol and methanol can accurately be predicted by van der Waals theory.

The thiol surfaces studied here exhibit a strong attraction in water. As different solvents are added, both the range of that attraction and the magnitude of the adhesion are decreased, with interactions being larger in ethylene glycol > methanol > ethanol. As discussed above, this phenomenon can be accounted for by the effect of the specific solvent on the contact angle measurements. Indeed, hexadecanethiol SAMs will be more solvophobic in ethylene glycol than in methanol or ethanol. As we also go from water to different solvents, we are changing the dielectric constant of the medium (80 for water, 41 for ethylene glycol, 33 for methanol, and 26 for ethanol (24)). It appears, therefore, that changes in the dielectric constant of the solvent track changes the contact angle of that solvent and as a consequence changes in the interaction forces between SAM surfaces can follow.

Note however that this is not the only mechanism by which hydrophobic forces can be altered. Previous studies have shown that as the electrolyte concentration in water is increased the strength of attractions increases between methyl-terminated SAM surfaces identical to those studied here (8). In this study, changes in contact angle with salt concentration could not be detected. Instead, a universal curve of adhesive force could be generated for different electrolyte types if the forces were plotted as a function of water–chemical potential. Comparing the effects of electrolyte and solvent type indicates that distinctly different mechanisms are at work in altering the magnitude of the hydrophobic force.

CONCLUSIONS

In this study we have demonstrated that the adhesive interactions of hydrophobic surfaces can be controlled in a systematic way by varying the solvent. The addition of solvents to aqueous solutions changes the dielectric constant of the medium and the contact angle of the solvent on the substrate. There is a clear connection between the effect of solvent on contact angle measurements, between the solvent and the surface of interest, and the effect of that solvent on the force profile of the SAM surfaces. This result is similar to that of

Rabinovich and Yoon (6) and Yoon *et al.* (7) who draw a similar conclusion based on holding the solvent constant and varying the surface composition. For the SAMs studied here, different solvents alter the solvent/surface interactions by changing the contact angles of the solutions on the surface in a reversible way, and results are sensitive to solvent type and concentration.

Adhesive forces and jump-in distances measured in the ethylene glycol–water system and in pure ethylene glycol, together with contact angle measurements of ethylene glycol on the SAM surface, showed that solvophobic interactions can be observed in both water and ethylene glycol and therefore cannot be attributed to the unique structural properties of water. Tsao *et al.* (29) also observed that long-range attractive forces were present in both water and ethylene glycol.

ACKNOWLEDGMENTS

We thank the Beckman Imaging Technology Group for the use of their Microscopy Suite Facility and the Center for Microanalysis of Materials for the use of their evaporator. This work was supported by NASA under Grant NAG8-1376, the Xerox Corporation, and the New Energy and Industrial Technology Development Organization on Integration of Materials by Solution Methods: Assembly at Reduced Temperatures.

REFERENCES

1. Ben-Naim, A., "Hydrophobic Interactions." Plenum, New York, 1980.
2. Adamson, A. W., and Gast, A., "Physical Chemistry of Surfaces." Wiley, New York, 1997.
3. Leja, J., "Surface Chemistry of Froth Flotation." Plenum, New York, 1982.
4. Drelich, J., Azevedo, M. A. D., Miller, J. D., and Dryden, P., *Prog. Paper Recycl.* **Aug.**, 31 (1996).
5. Zisman, W. A., in "Handbook of Adhesives" (I. Skeist, Ed.), Chap. 3. Van Nostrand, New York, 1977.
6. Rabinovich, Ya. I., and Yoon, R.-H., *Langmuir* **10**, 1903 (1994).
7. Yoon, R.-H., Flinn, D. H., and Rabinovich, Ya. I., *J. Colloid Interface Sci.* **185**, 363 (1997).
8. Kokkoli, E., and Zukoski, C. F., *Langmuir* **14**, 1189 (1998).
9. Bain, C. D., and Whitesides, G. M., *J. Am. Chem. Soc.* **110**, 3665 (1988).
10. Bain, C. D., Troughton, E. B., Tao, Y.-T., Evall, J., Whitesides, G. M., and Nuzzo, R. G., *J. Am. Chem. Soc.* **111**, 321 (1989).
11. Nuzzo, R. G., Dubois, L. H., and Allara, D. L., *J. Am. Chem. Soc.* **112**, 558 (1990).
12. Dubois, L. H., Zegarski, B. R., and Nuzzo, R. G., *J. Am. Chem. Soc.* **112**, 570 (1990).
13. Butt, H.-J., Seifert, K., and Bamberg, E., *J. Phys. Chem.* **97**, 7316 (1993).
14. Dubois, L. H., Zegarski, B. R., and Nuzzo, R. G., *J. Chem. Phys.* **98**, 678 (1993).
15. Rolandi, R., Cavalleri, O., Toneatto, C., and Ricci, D., *Thin Solid Films* **243**, 431 (1994).
16. Pan, W., Durning, C. J., and Turro, N. J., *Langmuir* **12**, 4469 (1996).
17. Frisbie, C. D., Rozsnyai, L. F., Noy, A., Wrighton, M. S., and Lieber, C. M., *Science* **265**, 2071 (1994).
18. Noy, A., Frisbie, C. D., Rozsnyai, L. F., Wrighton, M. S., and Lieber, C. M., *J. Am. Chem. Soc.* **117**, 7943 (1995).
19. Han, T., Williams, J. M., and Beebe, T. P., Jr., *Anal. Chim. Acta* **307**, 365 (1995).
20. Ducker, W. A., Senden, T. J., and Pashley, R. M., *Nature* **353**, 239 (1991).
21. Ducker, W. A., Senden, T. J., and Pashley, R. M., *Langmuir* **8**, 1831 (1992).
22. Cleveland, J. P., Manne, S., Bocek, D., and Hansma, P. K., *Rev. Sci. Instrum.* **64**, 403 (1993).
23. Liu, G., and Salmeron, M. B., *Langmuir* **10**, 367 (1994).
24. Israelachvili, J., "Intermolecular & Surface Forces." Academic Press, New York, 1992.
25. Derjaguin, B. V., *Kolloid Z.* **69**, 155 (1934).
26. Yaacobi, M., and Ben-Naim, A., *J. Solution Chem.* **2**, 425 (1973).
27. Parker, J. L., and Claesson, P. M., *Langmuir* **10**, 635 (1994).
28. Parker, J. L., Claesson, P. M., and Attard, P., *J. Phys. Chem.* **98**, 8468 (1994).
29. Tsao, Y.-H., Evans, D. F., and Wennerström, H., *Science* **262**, 547 (1993).
30. Parker, J. L., and Claesson, P. M., *Langmuir* **8**, 757 (1992).